The Role of Solutionizing Treatment on Microstructure, Mechanical and Corrosion Properties of AZ91 Magnesium Alloy

UDC:669.721:621.785
Original scientific paper https://doi.org/10.46793/aeletters.2026.11.3.2

Rajasekhara Babu Kankanala[1], Arun Kumar Lakshmi Narayanan[1], Ratna Sunil Buradagunta[2*]

[1]Department of Manufacturing Engineering, Annamalai University, Chidambaram 608002, India
[2]Department of Mechanical Engineering, Bapatla Engineering College, Bapatla 522101, India

Abstract:
In this research, AZ91 magnesium alloy was subjected to solutionizing at 410 °C for different soaking times (4, 8, 16, and 24 h), and the microstructure evolution, phase change, and mechanical and corrosion properties were investigated. From the microstructural studies, it was clearly observed that the intermetallic phase ($Mg_{17}Al_{12}$) appeared at the grain boundaries before heat treatment and was significantly altered after solutionizing. The X-ray diffraction studies after heat treatment clearly demonstrated a reduced fraction of intermetallic, which suggests the development of grains with super-saturated conditions due to the dissolved Al in the Mg lattice. Microhardness measurements showed decreased hardness (80.8 ± 2 HV0.1) with a lower level of variation within the measured values compared with the base alloy (93.6 ± 5.18 HV0.1). From the tensile test results, 8 h soaking time resulted in increased tensile strength up to 264.5 ± 6.1 MPa compared with the base alloy (171.6 ± 4.2 MPa) without sacrificing the % elongation. Further increasing the soaking time to 16 and 24 h did not improve the strength of the alloy. From the potentiodynamic polarization studies, lower corrosion current density values were observed for the samples with 8 and 16 h soaking time, which is attributed to the effect of lower intermetallic and homogeneous microstructure resulting from the heat treatment.

ARTICLE HISTORY
Received: 1 February 2026
Revised: 7 July 2026
Accepted: 3 August 2026
Published: 23 September 2026

KEYWORDS
Heat treatment, Magnesium, Microstructure, Mechanical properties, Corrosion

1. INTRODUCTION

Magnesium (Mg) alloys have gained tremendous interest among the non-ferrous alloys as promising candidates for lightweight components and structures [1, 2]. Among the commercially available Mg alloys, AZ series Mg alloys are widely used to manufacture engineering components and structures. Aluminium (Al) and zinc (Zn) are the principal alloying elements in AZ series alloys. With the addition of Al, formation of the intermetallic (Mg17Al12) phase is inevitable at room temperature [3, 4]. If Al content is increased to higher levels, a greater quantity of Mg17Al12 phase is produced and appears at the grain boundaries. Since the microstructure plays a significant role in the bulk behaviour of metals and alloys, altering the microstructure is a potential strategy in materials engineering [5, 6]. Heat treatment methods are widely adopted to enhance alloy performance by altering the microstructure. Solutionizing treatment increases the solubility of solute atoms in the solvent used to produce the alloys [7, 8]. Altering the phase fractions by heat treatment in alloys significantly improves the performance of engineering components.

AZ91 alloy is a cast alloy used to manufacture components and structures in the aircraft industry, automobile applications, and electric and electronic appliances [9]. Seat frames, steering frames, panels, gearbox components in automobile and aerospace, body structures, casings in laptops, and

*CONTACT: B. Ratna Sunil, e-mail: bratnasunil@gmail.com

construction structures in the sports and health care sector are the promising applications of AZ91 Mg alloy [10-12]. However, AZ91 Mg alloy shows poor formability, corrosion resistance and wear properties, which need to be addressed to enhance the performance of AZ91 Mg alloy to yield higher benefits in real-time applications [13, 14]. Usual heat treatments such as solutionizing (T4) and solutionizing followed by ageing (T6) are applied to AZ series Mg alloys [15]. Altering the microstructure can be a promising way to enhance alloy performance, as microstructure plays a very important role in bulk behaviour. Modifying the microstructure by mechanical processing has been demonstrated as a potential strategy to improve the formability, mechanical performance and corrosion behaviour of AZ91 alloy. Thermo-mechanical treatments such as multi-directional forging [16], snake rolling [17], accumulative back extrusion [18], micro-alloying and equal channel angular pressing (ECAP) [19] were successfully applied to alter the microstructure of AZ91 alloy. Among the reported mechanical processing methods, friction stir processing (FSP) was adopted by several authors to promote mechanical performance, wear resistance, corrosion resistance, and to improve the formability of AZ91 alloy [20-25].

On the other hand, heat treatment of Mg alloys was also demonstrated as a potential strategy to alter the microstructure [26-28]. The findings from the literature [29-31] demonstrated the significant role of the newly evolved microstructure in enhancing the bulk properties of Mg alloys. In earlier research [32], it was highlighted that solutionizing of AZ91 Mg alloy at 415 °C for 18 h introduced significant changes in the amount of intermetallic phase and increased the formability in hot working. During the heat treatment of AZ91 alloy, ageing also plays an important role. Fatmi et al. [33] investigated the mode of nucleation during ageing of AZ91 and observed that two modes of nucleation, including cellular and continuous modes, were the prime reasons behind the new microstructure evolution. Chowdary et al. [34] subjected AZ91 alloy to heat treatment at 410 °C for different soaking times (6, 12 and 24 h), and the decreased intermetallic content was observed as a prominent factor in improving the machinability during turning operation. Furthermore, from the corrosion studies, 6 and 12 h soaking times were observed with a similar effect on the corrosion rate. Huang et al. [35] solutionized AZ91 at three temperatures, 385 °C, 400 °C, and 415 °C, for 12 h of soaking time, and 415 °C was observed as a highly effective temperature to decrease the intermetallic phase and increase corrosion resistance and higher discharge voltage. Prem Kumar et al. [36] demonstrated that a soaking time of 8 to 12 h is sufficient to achieve full dissolution of the intermetallic phase. Srinivas et al. [37] also applied solutionizing to AZ91, and 12 h to 24 h soaking times gave increased mechanical properties and improved machinability properties. As per the SAE Standard AMS2768C, the recommended soaking time for solutioning of AZ91 at 410 - 418 °C is 16-24 h [38]. The solubility of Al in Mg gradually increases with increasing temperature, and at 437 °C, a maximum of 12.6 % can be reached [39]. Since AZ91 alloy has 9 % of Al, as recommended by SAE Standard AMS2768C [38], a soaking temperature between 410 and 418 °C is appropriate.

From the literature, it is understood that grain refinement by mechanical processing or by solutionizing treatment results in improved performance in AZ91 alloy. Based on the literature [34-36, 40, 41], it can be learnt that different solutionizing temperatures (above 400 °C) with different soaking times (2 to 120 h) significantly altered the microstructure. However, most of the works reported up to 24 h soaking time as highly influential on plastic deformation, fracture behaviour, mechanical strength, and corrosion properties of AZ91 alloy. However, the reported soaking times were inconsistent among the reported works, which is the prime objective of the current work. Therefore, AZ91 alloy was solutionized at 410 °C for 4, 8, 16, and 24 h, and the optimum soaking time was selected based on the criteria of maximum dissolution of the intermetallic phase. Then the effect of the newly evolved microstructure on the mechanical performance and corrosion resistance of the AZ91 alloy was investigated.

2. MATERIALS AND METHODS

AZ91 Mg alloy in the form of cast billets was procured from Exclusive Magnesium, Hyderabad, with a chemical composition of 9.1% Al, 0.96 % Zn, 0.1% and the remaining being Al by weight %. The samples were machined from the cast billet, and the surfaces were polished using emery papers (up to 2000 grade). Then, solutionizing treatment was carried out by heating the samples to 410 °C in a vacuum tubular furnace (VB Ceramics, India) with ± 2 °C accuracy for different soaking times (4, 8, 16 and 24 h) at a heating rate of 1.5 °C/min. Soaking was carried out in a protective atmosphere (Argon)

by continuously purging the heating chamber. Then the samples were collected from the furnace and immersed in water. Fig. 1a shows a typical heat treatment cycle adopted in the present study.

The heat treatment which gives solutionizing is called T4 treatment. Specimens (20 mm × 20 mm × 20 mm size) were heat treated for microstructural and phase analysis, corrosion and hardness measurements. For microstructural studies, the samples were polished with different graded emery papers (up to 2000 grade) followed by polishing using diamond paste (1-3 µm). The polished samples were cleaned with ethanol and then etched with Picric acid reagent with a chemical composition of 5 ml picric acid, 5 ml acetic acid, 5 ml water, and 100 ml ethanol. Etching was done by immersing the polished samples for 20 s. Samples of size as per ASTM E8 standard [42] as shown in Fig. 1b are machined from the billet and heat treated to evaluate the mechanical properties. The samples were coded as AZ91, AZ91 HT 4, AZ91 HT 8, AZ91 HT 16, and AZ91 HT 24 for base alloy and heat-treated alloys (4, 8, 16 and 24 h), respectively.

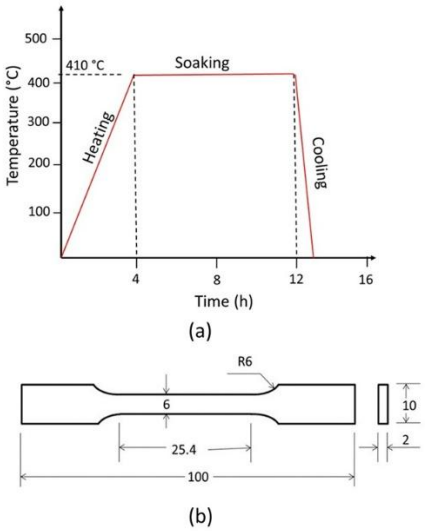

Fig. 1. (a) heat treatment cycle and (b) dimensions of tensile test samples (All dimensions are in mm)

For microstructural studies, samples were polished to a mirror-finishing level using an Olympus optical microscope (USA) by following metallographic procedures that included emery paper on a disc polishing machine, followed by diamond paste polishing. From the microstructures obtained from the centre of the heat-treated samples, the grain size of the samples was measured. Scanning electron microscopy (SEM) was performed using a TESCON device from the Czech Republic. Energy-dispersive X-ray analysis (EDS) was also performed on the base alloy to study the phase distribution. The polished surfaces were chemically etched (Picric acid reagent) and dried before obtaining the microstructures. X-ray diffractometry (XRD) was performed using a Bruker from the USA on the specimens (before and after heat treatment) for phase analysis in the range of 20° – 80° as 2θ value. The phase fraction (W_β) of $Mg_{17}Al_{12}$ in AZ91 alloy and HT samples was calculated by the reference intensity ratio (RIR) method using Eq. (1):

$$W_\beta = \frac{\frac{I_\beta}{K_\beta}}{\frac{I_\alpha}{K_\alpha}+\frac{I_\beta}{K_\beta}} \quad (1)$$

where: I_α is the (101) peak intensity of α-Mg and I_β is the (411) peak intensity of the $Mg_{17}Al_{12}$ phase from the XRD plot retrieved using Expert HighScore software, RIR constants, K_α for α-Mg is 1.44 (JCPDS file No. #35-0821) and K_β for $Mg_{17}Al_{12}$ is 1.05 (JCPDS #73-1148), were obtained from the International Centre for Crystallographic Data (ICDD).

Microhardness measurements were done by Vicker's microhardness method across the sample surface (at 100 g load), and the hardness number (HV0.1) was measured as per ASTM standard E384-22 [43]. Measurements were carried out on the polished samples (up to 2000-grade emery sheets). Ten measurements were carried out on each sample by keeping a 1 mm distance between each indent. The measurements were repeated three times (n=3), and the average values were compared. Tensile experiments were done at room temperature by applying a 0.01/s strain rate using a universal testing machine (UTM, Zwick-Roell from Germany) with an extensometer. From the measured load vs displacement data, stress-strain curves were drawn, and the tensile properties were compared. Three (n=3) experiments were done for each sample, and average values were obtained and compared.

Corrosion studies were carried out by potentiodynamic polarization (PDP) studies using a 3.5% NaCl solution in a test cell. The electrolyte (350 mL) was filled in the test cell, where 1 cm^2 of the workpiece was in contact with the electrolyte. Two electrodes, platinum (standard) and a saturated calomel electrode (reference), were used for the experiments. A scanning rate of 5 mV/s was used to record the electrochemical parameters. Open circuit potential (OCP) was observed for 30 min (exposure time), and PDP tests were carried out. From the obtained data, corrosion parameters (potential, E_{corr} and current density, i_{corr}) were recorded by Tafel extrapolation [44].

3. RESULTS AND DISCUSSION

The SEM image of AZ91 alloy and corresponding EDS analysis are presented in Fig 2. Usually, with higher Al content, the Mg17Al12 intermetallic in AZ-series Mg alloys appears significantly at the grain boundaries [45]. In the AZ91 alloy, higher Al content leads to the formation of the intermetallic as a network-like structure (Fig. 2a). The elemental composition of grains and grain boundaries indicated that the intermetallic was present at the grain boundaries with rich Al (Fig. 2b and 2c). Fig. 3 compares the microstructures of AZ91 and AZ91 HT samples (different soaking times). The three important regions of chemical heterogeneity in AZ91 are indicated in Fig. 3a. Among them, α-Mg is the region of solid solution grains formed by Mg (solvent) and Al (solute). The other two regions include the intermetallic region and the eutectic region adjacent to the intermetallic regions [46]. Due to the presence of more intermetallic and eutectic regions, AZ91 alloy exhibits higher brittleness compared with the other AZ series alloys (AZ31 and AZ61). The intermetallic phase is brittle and hard in nature. The solid solution grains exhibit a relatively soft nature, and the eutectic regions show moderate hardness. Therefore, altering these phase fractions and distribution by heat treatment significantly alters the bulk behaviour of the alloy. It is evident from the microstructures of AZ91 HT samples that solutionizing led to a substantial reduction in the intermetallic phase. The grain boundary regions, which are rich with the intermetallic before heat treatment, have undergone severe reduction in the fraction of the intermetallic, including the eutectic region. This observation suggests the increased solubility of Al in Mg, which was retained at room temperature. Increased Al dissolution into the soft α-phase causes grains to become rich with Al and, therefore, the development of supersaturated grains can be expected. After 8 h of soaking time, samples at 16 and 24 h exhibited little increase in solubility of the intermetallic phase, as observed from the microstructures.

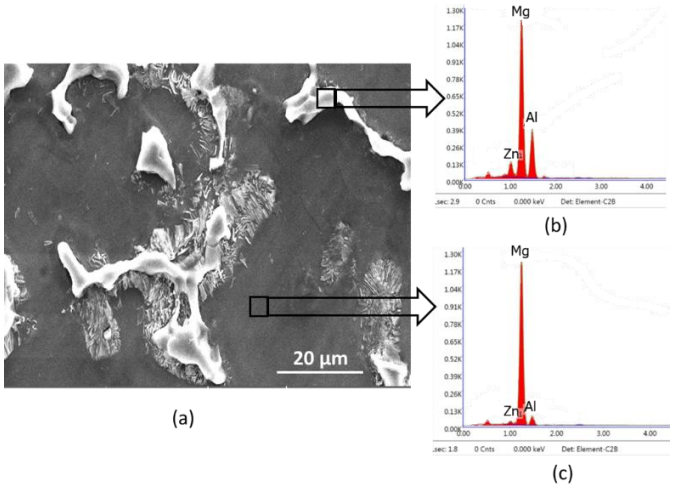

Fig. 2. SEM and EDS observations of AZ91 Mg alloy at different regions: (a) microstructure, (b) EDS spectra of intermetallic and (c) EDS analysis of a typical solid solution grain

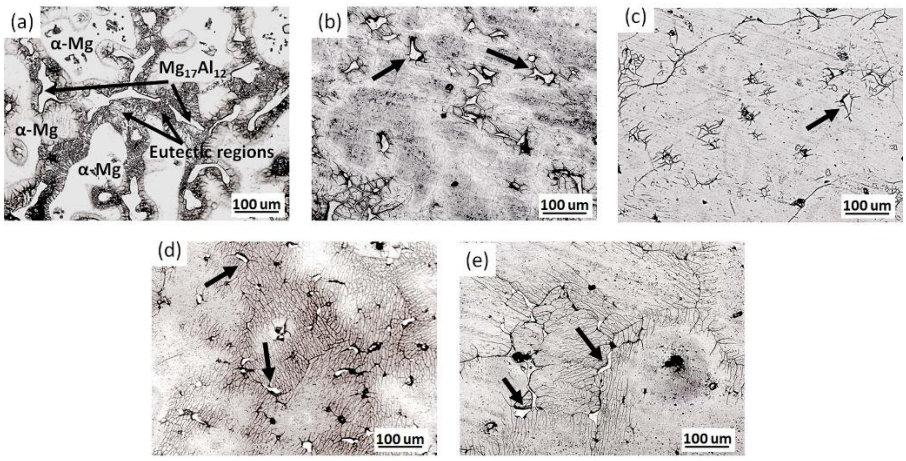

Fig. 3. Microstructures of the samples obtained from optical microscopy: (a) AZ91, (b) AZ91 HT 4, (c) AZ91 HT 8, (d) AZ91 HT 16 and (e) AZ91 HT 24

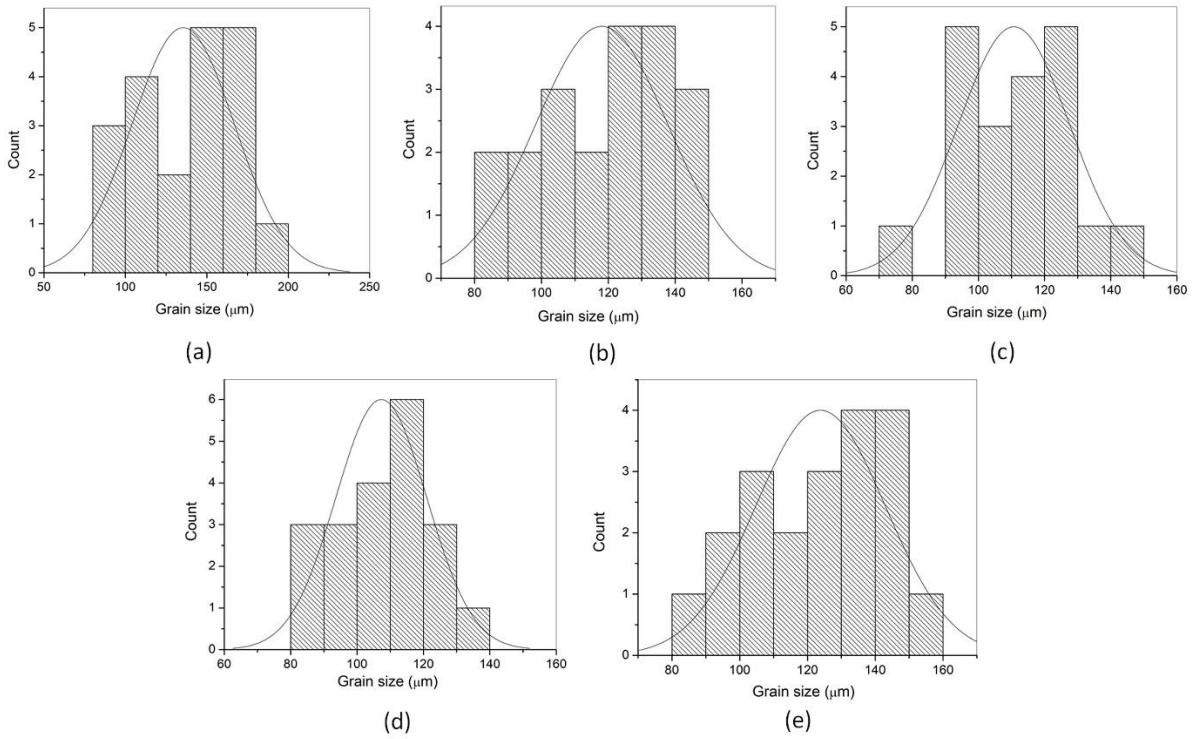

Fig. 4. Grain size distribution of the samples: (a) AZ91, (b) AZ91 HT 4, (c) AZ91 HT 8, (d) AZ91 HT 16 and (e) AZ91 HT 24

Fig. 4 compares the grain size measurements of the samples. The average grain size was determined by obtaining microstructures from the centre and the edge of the HT samples to ensure uniformity in the microstructure data.

At both locations (at the centre and at the surface), a similar kind of microstructure was observed in all the HT samples. Fig. 5 presents a typical microstructure of the AZ91 HT 8 sample obtained at the centre of the sample, indicating the grain boundaries and the presence of a lower intermetallic phase.

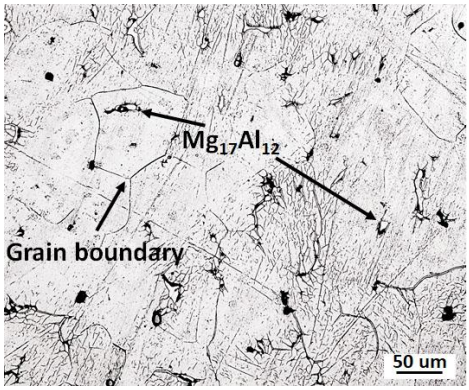

Fig. 5. Typical microstructure of AZ91 HT 8 sample

Grain size measurements were recorded as 135 ± 20.6 µm, 118.4 ± 19.4 µm, 110 ± 16.4 µm, 109 ± 14.8 µm, and 123 ± 18.7 µm for AZ91, AZ91 HT 4, AZ91 HT 8, AZ91 HT 16, and AZ91 HT 24, respectively. Statistically, ANOVA (Origin Pro8, USA) showed that, compared with the AZ91 sample, AZ91 HT 8 and AZ91 HT 16 samples had significantly different mean grain size values ($p<0.05$). Although the other samples (4 h and 24 h soaking time) showed marginally smaller grain sizes, the difference was not statistically significant at the $p<0.05$ level.

Fig. 6 presents the XRD plots of AZ91 and HT samples. All the peaks were indexed, and the two phases (α-Mg and $Mg_{17}Al_{12}$) were identified as shown in Fig 6 (a). No other peaks corresponding to any new phase were identified in the XRD of the AZ91 sample. Interestingly, after heat treatment, peak intensities corresponding to $Mg_{17}Al_{12}$ were significantly decreased for the HT, as shown in Fig. 6b. Particularly, up to 8 h, the intermetallic phase was significantly decreased, and for 16 and 24 h, similar levels of peak intensities were observed. In the AZ91 sample, 11.5 wt.% intermetallic phase was measured before HT. After 4 h of soaking time, the intermetallic phase decreased to 6.2 wt.%. For the AZ91 8 h sample, the fraction of intermetallic was decreased to 1.2 wt.%. Further, increasing the soaking time to 16 and 24 h resulted in values of 1 wt.% and 1.1 wt.%, respectively. As demonstrated by Alomairy [47], the dissolution of the $Mg_{17}A_{l2}$ phase occurs by atomic diffusion accompanied by interfacial interactions between the β-phase and α-Mg. The rate of diffusion of Al atoms in the Mg lattice within the solid state is controlled by slow diffusion; therefore, longer soaking time is required,

as explained by Zhu et al. [48]. Hence, as observed in the present work, longer soaking times of 8 and 16 h resulted in more dissolution of Al.

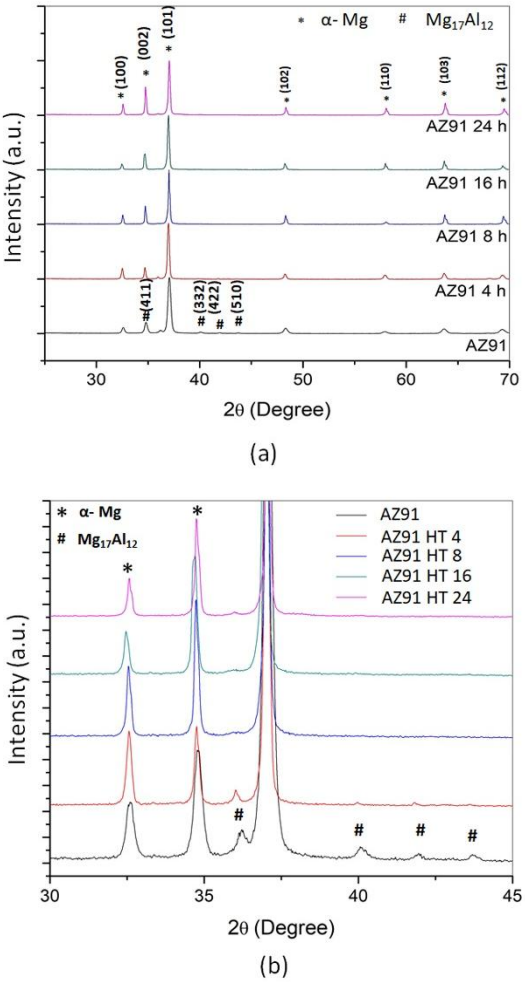

Fig. 6. XRD analysis of the samples : (a) comparison of all the samples and (b) specific 2θ range demonstrating decreased intermetallic phase

This finding, in correlation with microstructural studies, suggests that solutionizing decreased the intermetallic content by promoting more solubility of Al into Mg. Hence, from the microstructural characterisation and XRD analysis, the following two factors can be noted which significantly altered the bulk properties of AZ91 alloy.

i. Decreased intermetallic and eutectic zones next to the intermetallic phase
ii. Formation of grains with rich Al content (supersaturation) due to increased Al solubility

Fig. 7a shows the comparison of hardness data, and Fig. 7b presents the average values of the samples. From the hardness distribution values, greater variation was observed in the measured hardness values in the AZ91 sample. This can be explained by considering the contribution of hard and brittle intermetallic phases and eutectic zones. When the indent was placed on these regions, higher hardness was observed, as reported in the earlier work [49]. Whereas the solid-solution grains exhibited relatively lower hardness. Fig. 8 presents microstructures showing typical indents placed on the intermetallic phase (Fig. 8a) and on the soft α-Mg solid solution region (Fig 8.b). The size of the indents explains the higher hardness for the intermetallic phase and the lower hardness for the α-Mg regions. Therefore, more variations have been observed in the measured hardness values of AZ91. On the other hand, HT marginally decreased the hardness for all the samples.

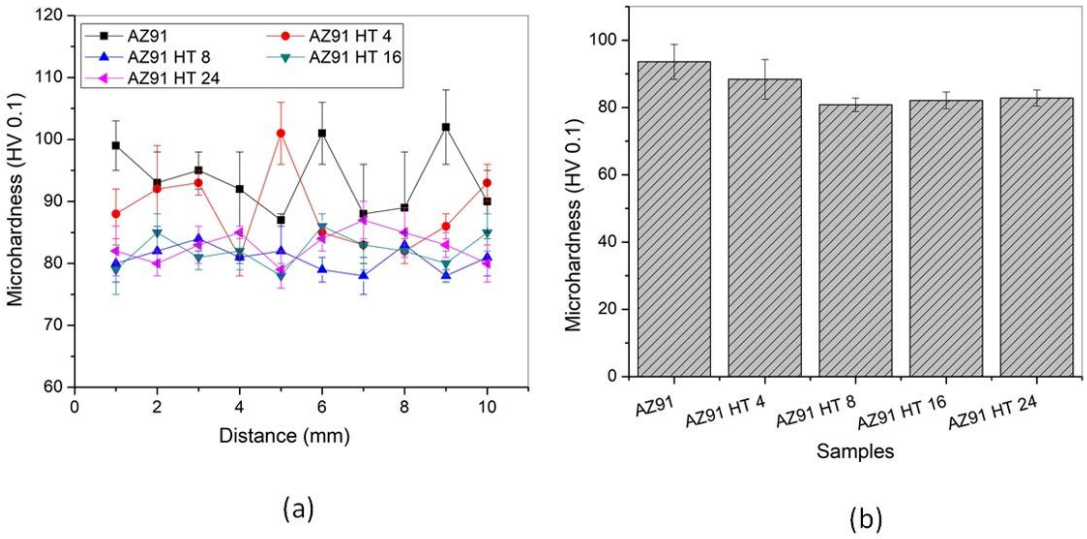

Fig.7. Hardness data of the samples: (a) distribution and (b) average values

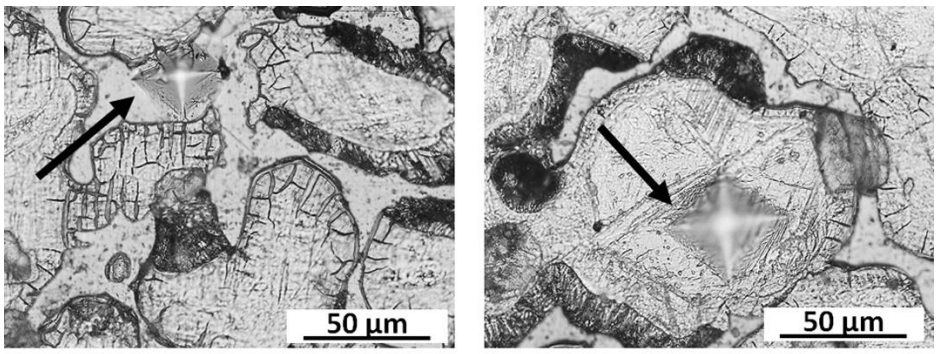

Fig. 8. Optical microscope images showing typical indents on AZ91 alloy at different regions (indicated with black arrows): (a) $Mg_{17}Al_{12}$ intermetallic phase and (b) solid solution grain (α-Mg)

For all the HT samples, the variations in the measured hardness were observed to be lower due to the increased homogeneity after HT. Interestingly, the average hardness was also observed to be decreased in the AZ91 HT sample. This observation is correlated with the altered phase fractions after heat treatment. Since the hard intermetallic phase was decreased by producing supersaturated grains, the reduction in hardness due to the decreased intermetallic is significant. Similarly, decreased regions of eutectic phase next to intermetallic also decrease the hardness after heat treatment. On the other hand, development of grains with increased Al solubility (supersaturation) leads to an increase in hardness. However, the reduction in hardness due to the lower intermetallic is dominant compared with the increased hardness due to supersaturated grains, and therefore the overall hardness of AZ91 HT samples was observed to decrease. However, at the $p<0.05$ level, the difference in the mean values was observed as statistically insignificant.

Fig. 9 presents the stress-strain curves of AZ91 and heat-treated samples obtained from tensile test results. Table 1 presents the tensile properties calculated from the test data. From the results, it is evident that AZ91 HT 8 and AZ91 HT 16 samples exhibited higher yield strength and ultimate tensile strength without sacrificing ductility, as reflected in marginally increased % elongation compared with the other samples. The increased strength after HT can be attributed to the developed solid-solution grains with a lower brittle nature resulting from the modified microstructure. The decreased intermetallic phase reduced the brittle nature, which helped to retain the ductility. When a solid solution alloy is formed by adding alloying elements, lattice distortion in the solid solution grains demands higher mechanical loads to initiate slip planes and achieve deformation, which is reflected as increased strength. Achieving increased strength and % of elongation together in AZ91 alloy by HT is a beneficial strategy to produce a high-performing AZ91 alloy. The tensile strength achieved in the current study is similar to values reported in previous studies. For example, Chen et al. [18] used accumulative back extrusion and an UTS value of 239. 23 MPa was achieved in AZ91 alloy. Similarly, Yousefpour et al. [21] reported improvement in UTS from 236.8 MPa to 267.1 MPa after FSP in AZ91 Mg alloy. In the current work, a lower UTS value (171.6 ± 4.2 MPa) was improved to 264.5 ± 6.1 MPa, which is within the same level of improvement. The results demonstrate that the benefit of implementing mechanical processing to enhance the performance of AZ91 alloy can be achieved by the HT process.

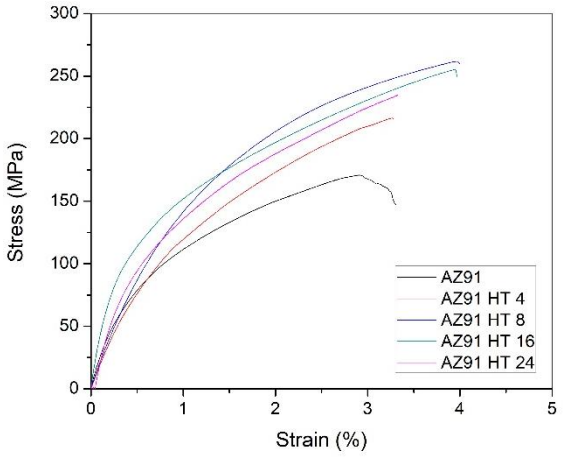

Fig. 9. Stress-strain curves of the samples

Table 1. Tensile properties of the samples

Sample	Yield strength (MPa)	Ultimate tensile strength (MPa)	% of elongation
AZ91	61.3 ± 3.5	168.5 ± 4.2	3.3 ± 1.1
AZ91 HT 4	63.5 ± 2.8	215.4 ± 5.3	3.2
AZ91 HT 8	104.6 ± 4.4	264.5 ± 6.1	4.1 ± 1.5
AZ91 HT 16	100.2 ± 3.1	253. 9 ± 4.8	3.9
AZ91 HT 24	86.3 ± 2.5	232.2 ± 4.5	3.2

Fig. 10 shows the comparison of PDP curves of the samples. The corrosion parameters obtained from the Tafel extrapolation are listed in Table 2. Lower i_{corr} values were observed for all HT samples compared with the AZ91 sample, which indicates better corrosion resistance after heat treatment. Among all the HT samples, AZ91 HT 8 and AZ91 HT 16 samples have shown relatively better corrosion resistance compared with AZ91 HT 4 and AZ91 HT 24 samples. Compared with the 16 h soaking time, the AZ91 HT 8 sample exhibited relatively better corrosion resistance. Usually, galvanic corrosion is seen in alloys which contain heterogeneous phases. Severe localised corrosion and pit formation are also influenced by the types of phases in contact in the presence of an electrolyte. If the difference in electrochemical potential between two phases is higher in the presence of a corroding electrolyte, galvanic corrosion is accelerated. In this work, the two important factors that helped increase the corrosion resistance of AZ91 HT are: a lower intermetallic phase, which decreased galvanic corrosion, and supersaturated grains, which reduced electrochemical activity [50]. The combined effect of these factors with the homogenised microstructure resulted in increased corrosion resistance of the AZ91 alloy after 8 and 16 h soaking times compared with the other soaking times.

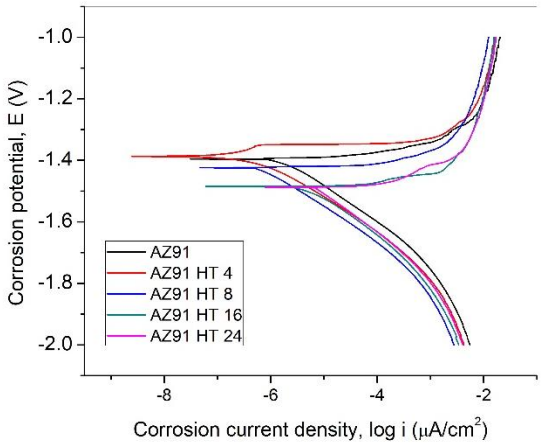

Fig. 10. PDP curves of the specimens

Table 2. Electrochemical data from the PDP curves of the samples

Samples	Corrosion potential, E_{corr} (V)	Corrosion current density, i_{corr} (mA/cm²)	Tafel slopes, (mV/decade)	
			β_a	β_c
AZ91	-1.38 ± 0.22	$3.61 \pm 0.85 \times 10^{-3}$	214.5 ± 25.2	285.3 ± 30.1
AZ91 HT 4	-1.37 ± 0.31	$3.99 \pm 0.42 \times 10^{-3}$	235.3 ± 30.6	301.5 ± 27.5
AZ91 HT 8	-1.42 ± 0.28	$1.35 \pm 0.53 \times 10^{-4}$	268.4 ± 33.6	325.6 ± 42.1
AZ91 HT 16	-1.49 ± 0.35	$1.70 \pm 0.55 \times 10^{-4}$	266.3 ± 28.1	312.9 ± 36.7
AZ91 HT 24	-1.48 ± 0.23	$4.22 \pm 0.46 \times 10^{-3}$	231.6 ± 22.5	298.2 ± 35.4

AZ91 Mg alloy is a cast alloy and exhibits a heterogeneous microstructure with a distribution of hard intermetallic and soft solid solution grains. Several engineering applications use cast-AZ91 structures due to the lower weight and higher specific strength. However, subjecting AZ91 to a suitable heat treatment to alter the microstructure to improve mechanical and corrosion properties is a promising strategy as demonstrated in the current work. Heat treatment is a simple process and can be carried out conveniently by using the existing industrial furnaces. Therefore, adopting solutionizing treatment to decrease the fraction of intermetallic and to produce super-saturated grains can be applied to the engineering components made of AZ91 alloy. It can be summarized that heat-treated AZ91 alloy can be used to manufacture components and structures with enhanced mechanical and corrosion performance. If improving the mechanical performance is the criterion behind the selection of the soaking time, 8 or 16 h is suggested. If the structure is intended to work in a corrosive environment, an 8 h soaking time is suggested.

4. CONCLUSION

In the current research work, AZ91 alloy was solutionized at 410 °C for 4, 8, 16 and 24 h to introduce microstructural changes, and then the role of heat treatment on mechanical performance and corrosion properties was studied. From the results, the following conclusions can be drawn.

i. Up to 8 h soaking time, significant microstructural changes were observed and increasing the soaking time further to 16 and 24 h resulted in not much change in the microstructure.
ii. From the XRD analysis of AZ91 and all HT samples, decreased $Mg_{17}Al_{12}$ phase and also eutectic regions were observed, which suggests higher solubility of Al that led to the production of grains with supersaturation.
iii. Microhardness measurements demonstrated decreased hardness (80.8 ± 2 HV0.1) for the solutionized alloys compared with the pre-treatment condition (93.6 ± 5.18 HV0.1). However, the variations were observed as a decrease in heat-treated samples, which is attributed to the homogeneous microstructure resulting from the solutionizing treatment.
iv. Tensile test results clearly demonstrated increased strength up to 264.5 ± 6.1 MPa for the solutionized alloy (8 h soaking time), which is higher than AZ91 (171.6 ± 4.2 MPa) without losing the ductility, as reflected by the similar % elongation for both samples. Similar tensile behaviour was also noticed after 16 h of soaking time. Further increasing the soaking time to 24 h did not result in higher tensile properties.
v. Corrosion studies carried out by potentiodynamic polarization tests indicated lower i_{corr} values for the solutionized alloys due to the decreased galvanic corrosion and increased homogeneous microstructure. Among all the HT samples, the AZ91 HT 8 sample exhibited better corrosion resistance.

From the overall observations, it can be concluded that solutionizing at 410 °C for 8 and 16 h of soaking time helps significantly alter the microstructure in AZ91 alloy to enhance the mechanical and corrosion properties, which are essentially useful for producing high-performing structures in automobile, aerospace, and electronic goods applications. Considering the mechanical performance of the alloy, 8 or 16 h soaking time can be adopted. If corrosion resistance is the objective behind heat treatment, an 8 h soaking time is suggested to achieve better corrosion performance for AZ91 alloy.

CONFLICTS OF INTEREST

The authors declare no competing interests.

REFERENCES

[1] J. Zhang, J. Miao, N. Balasubramani, D.H. Cho, T. Avey, C.-Y. Chang, A.A. Luo, Magnesium research and applications: Past, present and future. *Journal of Magnesium and Alloys*, 11(11), 2023: 3867-3895. https://doi.org/10.1016/j.jma.2023.11.007

[2] R.L. Edgar, Global overview on demand and applications for magnesium alloys, In: *Magnesium Alloys and their Applications*, K.U. Kainer (ed.), Wiley-VCH, Germany, 2000: 1-8. https://doi.org/10.1002/3527607552.ch1

[3] S. Jayasathyakawin, M. Ravichandran, N. Baskar, C. Anand Chairman, R. Balasundaram, Mechanical properties and applications of Magnesium alloy–Review. *Materials Today: Proceedings*, 27, 2020: 909-913. https://doi.org/10.1016/j.matpr.2020.01.255

[4] Y. Narukawa, K. Watanabe, K. Matsuda, T. Kawabata, S. Ikeno, Effect of Zn Contents on Microstructure in AZ-Series Magnesium Alloys. *Advanced Materials Research*, 409, 2011: 358–361. https://doi.org/10.4028/www.scientific.net/AMR.409.358

[5] J. Ma, G. Wang, Y. Li, C. Qin, F. Ren, Electrochemical Investigations on AZ Series Magnesium Alloys as Anode Materials in a Sodium Chloride Solution. *Journal of Materials Engineering and Performance*, 28, 2019: 2873–2880. https://doi.org/10.1007/s11665-019-04035-w

[6] C. Ma, C. Hou, X. Zhang, T. Liu, N. Zhou, K. Zheng, Study on the microstructure and mechanical properties of Mg–Al–Li–Zn–Ti multi-component alloy. *Journal of Materials Research and Technology*, 29, 2024: 4781-4795. https://doi.org/10.1016/j.jmrt.2024.02.171

[7] C. Frank, W. Kasprzak, Heat Treatment of Magnesium Alloys – Current Capabilities. *Materials Science Forum*, 765, 2013: 466-470. https://doi.org/10.4028/www.scientific.net/MSF.765.466

[8] A. Pandya, M. Shah, B. Pramod, N. Srivastava, A Review on Heat Treatment of Magnesium Alloys and Its Effect on Various Properties. In: P.B. Pramod, U.B. Desai, S. Goel (Eds.),

Advances in Material Science and Metallurgy. *Lecture Notes in Mechanical Engineering*, Springer, Singapore, 2023: 77-87. https://doi.org/10.1007/978-981-19-4918-0_7

[9] G.G. Wang, J.P. Weiler, Recent developments in high-pressure die-cast magnesium alloys for automotive and future applications. *Journal of Magnesium and Alloys*, 11(1), 2023: 78-87. https://doi.org/10.1016/j.jma.2022.10.001

[10] J. Tan, S. Ramakrishna, Applications of magnesium and its alloys: a review. *Applied Sciences*, 11(15), 2021: 6861. https://doi.org/10.3390/app11156861

[11] V.V. Ramalingam, P. Ramasamy, M.D. Kovukkal, G. Myilsamy, Research and development in magnesium alloys for industrial and biomedical applications: a review. *Metals and Materials International*, 26(4), 2020: 409-430. https://doi.org/10.1007/s12540-019-00346-8

[12] H. Xie, H. Zhao, X. Guo, Y. Li, H. Hu, J. Song, B. Jiang, F. Pan, Recent progress on cast magnesium alloy and components. *Journal of Materials Science*, 59, 2024: 9969-10002. https://doi.org/10.1007/s10853-024-09459-x

[13] B.C. Pai, U.T.S. Pillai, P. Manikandan, A. Srinivasan, Modification of AZ91 Mg alloys for high temperature applications. *Transactions of the Indian Institute of Metals*, 65, 2012: 601-606. https://doi.org/10.1007/s12666-012-0166-1

[14] J. Iwaszko, M. Strzelecka, Microstructure and Corrosion Resistance of AZ91 Magnesium Alloy after Surface Remelting Treatment. *Materials*, 15(24), 2022: 8980. https://doi.org/10.3390/ma15248980

[15] G.E. Totten, Heat Treating of Nonferrous Alloys. *ASM International*, 4E, 2016: 640-649. https://doi.org/10.31399/asm.hb.v04e.a0006254

[16] M. Şahbaz, S. Nalkıran, Microstructural refinement and mechanical property enhancement of AZ91 magnesium alloy via room-temperature multi-directional forging. *Scientific Reports*, 16, 2026: 9745. https://doi.org/10.1038/s41598-026-42311-7

[17] C. Dong, L.-H. Pang, Y. Li, C. Xu, Effect of offset distance on the microstructure and properties of AZ91 magnesium alloy sheets processed by snake rolling. *Materials Letters*, 410, 2026: 140285. https://doi.org/10.1016/j.matlet.2026.140285

[18] C. Chen, Y. Xu, H. Zhang, M. Zhang, J. Jia, J. Li, S. Chen, F. Wang, Grain refinement and β phase dispersion of AZ91D magnesium alloy by accumulative back extrusion: microstructure and mechanical properties. *Journal of Materials Research and Technology*, 37, 2025: 4176-4188. https://doi.org/10.1016/j.jmrt.2025.07.112

[19] K. Wan, Q. Xu, Q. Hu, A. Wang, K. Hu, Y. Li, D. Yang, A. Ma, J. Jiang, Synergistic optimization of corrosion resistance in AZ91 alloy by lanthanum microalloying and equal-channel angular pressing. *Journal of Rare Earths*, 2026. (In Press). https://doi.org/10.1016/j.jre.2026.03.023

[20] G.V.V. Surya Kiran, K. Hari Krishna, S. Sameer, M. Bhargavi, B.S. Kumar, G. Mohana Rao, Y. Naidubabu, R. Dumpala, B.R. Sunil, Machining characteristics of fine grained AZ91 Mg alloy processed by friction stir processing. *Transactions of Nonferrous Metals Society of China*, 27(4), 2017: 804-811. https://doi.org/10.1016/S1003-6326(17)60092-X

[21] F. Yousefpour, R. Jamaati, H. J. Aval, Effect of traverse and rotational speeds on microstructure, texture, and mechanical properties of friction stir processed AZ91 alloy. *Materials Characterization*, 178, 2021: 111235. https://doi.org/10.1016/j.matchar.2021.111235

[22] B.M. Hasani, H. Hedaiatmofidi, A. Zarebidaki, Effect of friction stir process on the microstructure and corrosion behavior of AZ91 Mg alloy. *Materials Chemistry and Physics*, 267, 2021: 124672. https://doi.org/10.1016/j.matchemphys.2021.124672

[23] J. Iwaszko, K. Kudła, Microstructure, hardness, and wear resistance of AZ91 magnesium alloy produced by friction stir processing with air-cooling. *The International Journal of Advanced Manufacturing Technology*, 116(3), 2021: 1309-1323. https://doi.org/10.1007/s00170-021-07474-9

[24] K.J. Sandeep, A.K. Choudhary, R.J. Immanuel, Microstructural characterization and mechanical performance of AZ91 magnesium alloy processed by friction stir processing using novel tool designs. *Journal of Materials Engineering and Performance*, 33(1), 2024: 120-135. https://doi.org/10.1007/s11665-023-07980-9

[25] S.K. Baral, M.M. Thawre, B.R. Sunil, R. Dumpala, Synergetic Effect of Ball Burnishing and Friction Stir Processing on the Sliding Wear Behavior of ZE41 Magnesium Alloy. *Journal of Materials*

Engineering and Performance, 35(4), 2026: 3978-3988. https://doi.org/10.1007/s11665-025-11855-6

[26] Y. Guo, G. Quan, M. Celikin, L. Ren, Y. Zhan, L. Fan, H. Pan, Effect of heat treatment on the microstructure and mechanical properties of AZ80M magnesium alloy fabricated by wire arc additive manufacturing. *Journal of Magnesium and Alloys*, 10(7), 2022: 1930-1940. https://doi.org/10.1016/j.jma.2021.04.006

[27] A.K. Alfozan, Effect of Heat Treatment on Formability of AZ61 Magnesium Alloys. *Solid State Phenomena*, 356, 2024: 15-20. https://doi.org/10.4028/p-Bw1228

[28] R.S. Buradagunta, Synergic effect of grain refinement and solutionizing on mechanical properties and corrosion behavior of ZE41 Mg alloy aimed for biomedical applications. *Materials Research Express*, 13(1), 2026: 015401. https://doi.org/10.1088/2053-1591/ae30d3

[29] N. Najm, A.H. Ataiwi, R.A. Anaee, Annealing and Coating Influence on the Mechanical Properties, Microstructure, and Corrosion Properties of Biodegradable Mg Alloy (AZ91). *Journal of Bio- and Tribo-Corrosion*, 8, 2022: 64 https://doi.org/10.1007/s40735-022-00662-4

[30] N. Najm, A. H. Ataiwi, R. A. Anaee, Effect of indium coating on corrosion behavior of AZ31 Mg alloy by DC Sputtering. *Materials Today: Proceedings*, 62, 2022: 4551–4555. https://doi.org/10.1016/j.matpr.2022.05.241

[31] N. Najm, A.H. Ataiwi, R.A. Anaee, R.S.A. Adnan, The effect of solid solution treatment with coating on corrosion properties of AZ91 Mg alloy in simulated body fluid. *Materials Today: Proceedings*, 2023. https://doi.org/10.1016/j.matpr.2023.10.009

[32] L. Cizek, M. Greger, L. Pawlica, L. A. Dobrzanski, T. Tanski, Study of selected properties of magnesium alloy AZ91 after heat treatment and forming. *Journal of Materials Processing Technology*, 157-158, 2004: 466–471. https://doi.org/10.1016/j.jmatprotec.2004.07.149

[33] M. Fatmi, A. Djemli, A. Ouali, T. Chihi, M.A. Ghebouli, H. Belhouchet, Heat treatment and kinetics of precipitation of β-Mg17Al12 phase in AZ91 alloy. *Results in Physics*, 10, 2018: 693-698. https://doi.org/10.1016/j.rinp.2018.07.009

[34] V.S. Chowdary, R. Dumpala, S. Anand Kumar, V. V. Kondaiah, B. Ratna Sunil, Influence of heat treatment on the machinability and corrosion behavior of AZ91 Mg alloy. *Journal of Magnesium and Alloys*, 6(1), 2018: 52-58. https://doi.org/10.1016/j.jma.2017.12.001

[35] Z. Huang, Y. Pei, R. Huang, X. Gao, J. Zou, L. Jiang, Effect of Solution-treated on Electrochemical Properties of AZ91 Magnesium Alloy Anode. *Journal of Electrochemical Science and Technology*, 13(4), 2022: 486-496. https://doi.org/10.33961/jecst.2022.00430

[36] S. Prem Kumar, S. Kumaran, T. Srinivasa Rao, Structure – property correlation of precipitation hardened AZ91 magnesium alloy. *Materials Science and Technology*, 20(7), 2004: 835-838. https://doi.org/10.1179/026708304225017256

[37] A. Srinivas, D. Pavan, B.K. Venkatesha, R. Raghavendra Rao, L. Mohith, Study on mechanical properties of AZ91 magnesium alloy. *Materials Today: Proceedings,* 54, 2022: 291-294. https://doi.org/10.1016/j.matpr.2021.09.171

[38] SAE International Material Specification, Heat Treatment of Magnesium Alloy Castings. *SAE Standard AMS2768C*, USA, 2005. https://doi.org/10.4271/AMS2768C

[39] B.L. Mordike, T. Ebert, Magnesium: Properties - applications — potential. *Materials Science and Engineering: A*, 302(1), 2001: 37-45. https://doi.org/10.1016/S0921-5093(00)01351-4

[40] Z.-y. You, A.-x. Jiang, Z.-z. Duan, G.-p. Qiao, J.-l. Gao, L.-b. Guo, Effect of heat treatment on microstructure and properties of semi-solid squeeze casting AZ91D. *China Foundry*, 17, 2020: 219–226. https://doi.org/10.1007/s41230-020-9103-9

[41] R. Sarvesha, D. Chalapathi, M. Yadava, J. Jain, S.S. Singh, In-situ studies on deformation and fracture characteristics of AZ91 Mg alloy. *Materialia*, 18, 2021: 101177. https://doi.org/10.1016/j.mtla.2021.101177

[42] ASTM E8/E8M-22, Standard Test Methods for Tension Testing of Metallic Materials. *ASTM International*, West Conshohocken, PA, USA, 2022. https://doi.org/10.1520/E0008_E0008M-22

[43] ASTM E384-22, Standard Test Method for Microindentation Hardness of Materials. *ASTM International*, West Conshohocken, PA, USA, 2022. https://doi.org/10.1520/E0384-22

[44] F. Mansfeld, The polarization resistance technique for measuring corrosion currents, In: M.G. Fontana, R.W. Staehle, (Eds.). Advances in Corrosion Science and Technology. *Springer*, Boston, USA, 1976: 163-262. https://doi.org/10.1007/978-1-4684-8986-6_3

[45] M. Avedesian, H. Baker, ASM Specialty Handbook: Magnesium and Magnesium Alloys. *ASM International*, USA, 1999.

[46] Z.U. Rehman, J.S. Kim, D.G. Churchill, B.H. Koo, Tuning Corrosion Properties of the Bio-Inspired AZ-Series Mg Alloys Using Electrochemical Surface Treatment under Varying Experimental Regimes. *Coatings*, 12(11), 2022: 1617. https://doi.org/10.3390/coatings12111617

[47] S. Alomairy, Dissolution mechanism and kinetics of β(Mg17Al12) phases in AZ91 magnesium alloy. *Journal of Magnesium and Alloys*, 12(4), 2024: 1581-1592. https://doi.org/10.1016/j.jma.2024.03.020

[48] T. Zhu, Z. Chen, W. Gao, Dissolution of Eutectic β-Mg17Al12 Phase in Magnesium AZ91 Cast Alloy at Temperatures Close to Eutectic Temperature. *Journal of Materials Engineering and Performance*, 19, 2009: 860-867. https://doi.org/10.1007/s11665-009-9539-y

[49] B.R. Sunil, K.V. Ganesh, P. Pavan, G. Vadapalli, Ch. Swarnalatha, P. Swapna, P. Bindukumar, G.P.K. Reddy, Effect of aluminium content on machining characteristics of AZ31 and AZ91 magnesium alloys during drilling. *Journal of Magnesium and Alloys*, 4(1), 2016: 15-21. https://doi.org/10.1016/j.jma.2015.10.003

[50] P.-P. Wu, G.-L. Song, Y.-X. Zhu, Z.-L. Feng, D.-J. Zheng, The corrosion of Al-supersaturated Mg matrix and the galvanic effect of secondary phase nanoparticles. *Corrosion Science*, 184, 2021: 109410. https://doi.org/10.1016/j.corsci.2021.109410

© 2026 by the authors. This work is licensed under a Creative Commons Attribution-Non Commercial 4.0 International License (CC BY-NC 4.0).